52nd IEEE Conference on Decision and Control
December 10-13, 2013. Florence, Italy

Controller Design of a Grid-tie Inverter bypassing DQ transformation

Yoshito Ohta* , Akihiro Ohori**, Nobuyuki Hattori** , and Kenji Hirata***

Abstract— **This paper proposes a novel approach for the controller design of a three-phase grid-tie inverter. First, the paper analyzes the input-output map of the system consisting of the cascade connection of a diagonal transfer function pre- and post-multiplied by DQ (direct-quadrature) and inverse DQ transformations which are prevalently used as a controller for systems with a rotating axis. It shows that the input-output map is time invariant when the angular velocity of DQ transformation is constant and derives the transfer function. It extends the result when the angular velocity is not constant, and derives an LPV state-space representation of the input-output map. Second, the paper analyzes the input-output map in terms of the positive and negative phase sequence components. Finally, the paper applies the analysis to the controller design for a grid-tie inverter bypassing DQ transformation. The efficacy of the proposed method is verified by a simulation and an experiment.**

I. INTRODUCTION

The use of renewable energy for electric power generation is growing to meet the demand for low-carbon emission and sustainable production. Many national and local governments set goals for renewable energy. For example, the state of California requires renewables will be required to account for more than 33% in 2020 [1]. The Japanese government aims to introduce nearly 30% of renewables by 2030 [2].

Variable energy resources such as solar and wind produce no green house gases. Photovoltaic (PV) power generation especially has several advantages: it is free from air pollutants or noise, it has no mechanical corrosion, and it can be installed at various places. On the other hand, PV generation is suseptible to weather conditions.

PV systems are connected to a low (medium) voltage grid through grid-tie inverters. Many countries and regions impose connection standards for grid-tie inverters such as IEEE 1547 [3], [4], G83/1-1 [5], BDEW Technical Guideline [6], and JESC E0019 (2012) [7]. With the increase of distributed generators, inverters are subject to stricter rules for connection and/or disconnection. Some rules specify fault detection, identification, and recovery standards. For example, when the grid undergoes voltage drop, frequency change, frequency rate change inverters have to satisfy Fault Ride Through (FRT) capabilities.

The controller design problem for grid-tie inverters should address the following requirements; (a) inverters meet connection standards such as FRT requirements, and (b) inverters are able to control voltage and frequency fluctuations caused by weather conditions. This necessitates that the controller should materialize fast response as well as robustness against perturbations.

A conventional controller configuration is the cascade connection of a diagonal transfer function pre- and post-multiplied by DQ and inverse DQ transformations [8], [9]. The elements of the diagonal transfer function are called single-phase compensators, and are mostly chosen from the class of low pass filters and PI controllers. DQ transformation maps sinusoidal signals into direct current (DC) signals, and it makes sense to design the system to track a set point. Though this is intuitively appealing, how to select filter parameters and PI gains to improve the control performance is not transparent because DQ transformation is a time varying transformation. In [10], a PR controller is constructed from a PI controller using lowpass-highpass transformation, where R is for resonance in PR. However, lowpass-highpass transformation does not fully explain the role of DQ transformation.

This paper proposes a novel approach for the controller design problem of a grid-tie inverter bypassing DQ transformation. First, we show that the cascade connection of DQ transformation, a transfer function, and the inverse transformation is equivalent to a linear time-invariant system having a certain structure. Furthermore, the result is extended to the situation where the angle velocity is not constant. Second, we analyze the effect of positive phase and negative phase signals by the transfer function. Third, we decide the weighting transfer function for the H^∞ loop shaping approach [11] using the new findings in this paper. Finally, we demonstrate by a simulation and an experiment that the design method is effective to construct a controller that achieves FRT capabilities required by JESC E0019 (2012).

II. DQ TRANSFORMATION

A. Clarke transformation and DQ transformation

The analysis of a three-phase AC (alternating current) system exploits Clarke and DQ transformations. Clarke transformation studied in [12] transforms three-phase signals u_a, u_b, u_c to two-phase signals u_α, u_β via[1]

$$\begin{bmatrix} u_\alpha \\ u_\beta \\ u_0 \end{bmatrix} = \sqrt{\frac{2}{3}} \begin{bmatrix} 1 & -\frac{1}{2} & -\frac{1}{2} \\ 0 & \frac{\sqrt{3}}{2} & -\frac{\sqrt{3}}{2} \\ \frac{1}{\sqrt{2}} & \frac{1}{\sqrt{2}} & \frac{1}{\sqrt{2}} \end{bmatrix} \begin{bmatrix} u_a \\ u_b \\ u_c \end{bmatrix}.$$

* Y.Ohta is with Department of Applied Mathematics and Physics, Kyoto University, Kyoto, 606-8501, Japan, E-mail yoshito_ohta@i.kyoto-u.ac.jp

** A.Ohori and N.Hattori are with DAIHEN corporation, 2-1-11 Tagawa, Yodogawa-ku, Osaka, Japan

*** K.Hirata is with Nagaoka University of Technology, 1603-1, Kamitomioka, Nagaoka, Niigata 940-2188, Japan

[1]The reference [12] uses a different scaling factor. The transformation matrix in this paper is scaled to be normalized.

978-1-4673-5716-6/13/$31.00 ©2013 IEEE

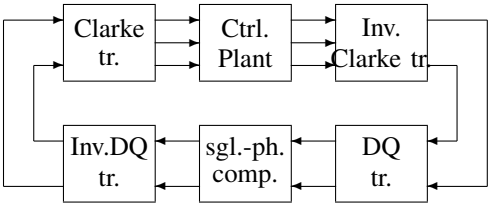

Fig. 1. DQ transformation and single-phase compensator

Notice that $u_0 = 0$ if the three-phase signal is balanced, *i.e.*, $u_a + u_b + u_c = 0$. This is also called three-phase two-phase transformation. The inverse transform that maps u_α, u_β (and u_0) to u_a, u_b, and u_c is called two-phase three-phase transformation.

If the signals u_a, u_b, and u_c are sinusoidal with the phase difference $2\pi/3$, *i.e.*,

$$u_a = \sqrt{2}U \sin\left(\theta(t) - \delta\right), \tag{1}$$

$$u_b = \sqrt{2}U \sin\left(\theta(t) - \delta - \frac{2\pi}{3}\right), \tag{2}$$

$$u_c = \sqrt{2}U \sin\left(\theta(t) - \delta - \frac{4\pi}{3}\right), \tag{3}$$

with $\theta(t) = \omega_0 t$, then

$$u_\alpha = \sqrt{3}U \sin\left(\theta(t) - \delta\right), \tag{4}$$

$$u_\beta = \sqrt{3}U \sin\left(\theta(t) - \delta - \frac{\pi}{2}\right), \tag{5}$$

so the signals u_α and u_β are sinusoidal with the phase difference $\pi/2$.

DQ transformation is originally used to analyze and control synchronous machines [13]. Two-phase signals u_α, u_β are transformed via

$$\begin{bmatrix} u_d \\ u_q \end{bmatrix} = \begin{bmatrix} \cos\theta(t) & \sin\theta(t) \\ -\sin\theta(t) & \cos\theta(t) \end{bmatrix} \begin{bmatrix} u_\alpha \\ u_\beta \end{bmatrix}. \tag{6}$$

We call u_d as the direct-axis component, and u_q as the quadrature-axis component, and the name DQ transformation (direct-quadrature-transformation). If the two-phase signals are given by (4) and (5), then

$$u_d = -\sqrt{3}U \sin\delta, \quad u_q = -\sqrt{3}U \cos\delta,$$

and the direct-axis and quadrature-axis components are both constant signals.

B. Equivalent system – constant angular velocity

A conventional feedback structure for a three-phase system is shown in Fig. 1. The three-phase signals are transformed by Clarke transformation, and the two-phase signals are transformed by DQ transformation. The direct-axis and quadrature-axis components are fed to a common single-phase compensator. Then the signals are transformed back by the inverse DQ and Clarke transformations.

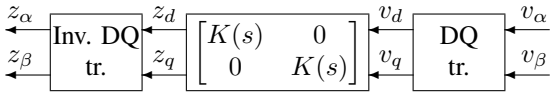

Fig. 2. Cascade connection of DQ transformation and a single-phase diagonal transfer function

The bottom row of Fig. 1 is depicted in Fig. 2. Note that the transformation matrix in (6) satisfies

$$\begin{bmatrix} \cos\theta & \sin\theta \\ -\sin\theta & \cos\theta \end{bmatrix} = T \begin{bmatrix} e^{j\theta} & 0 \\ 0 & e^{-j\theta} \end{bmatrix} T^{-1} \tag{7}$$

$$T = \frac{1}{2}\begin{bmatrix} 1 & 1 \\ j & -j \end{bmatrix}, \quad T^{-1} = \begin{bmatrix} 1 & -j \\ 1 & j \end{bmatrix}.$$

In this subsection, the signals (1), (2), and (3) satisfy $\theta(t) = \omega_0 t$ for some $\omega_0 > 0$. For the sake of simplicity, we assume that signals are scalar valued. An extension for vector signals is straightforward. Define signals using (7):

$$\begin{bmatrix} \tilde{v}_\alpha \\ \tilde{v}_\beta \end{bmatrix} = T^{-1} \begin{bmatrix} v_\alpha \\ v_\beta \end{bmatrix}, \quad \begin{bmatrix} \tilde{z}_\alpha \\ \tilde{z}_\beta \end{bmatrix} = T^{-1} \begin{bmatrix} z_\alpha \\ z_\beta \end{bmatrix},$$

$$\begin{bmatrix} \tilde{v}_d \\ \tilde{v}_q \end{bmatrix} = T^{-1} \begin{bmatrix} v_d \\ v_q \end{bmatrix}, \quad \begin{bmatrix} \tilde{z}_d \\ \tilde{z}_q \end{bmatrix} = T^{-1} \begin{bmatrix} z_d \\ z_q \end{bmatrix}.$$

Because the diagonal transfer function $\mathrm{diag}\,\{K(s), K(s)\}$ commutes with T, Fig. 2 is replaced by Fig. 3, where the multiplication and the inverse-multiplication mean that signals are multiplied by the matrices

$$\begin{bmatrix} e^{j\theta(t)} & 0 \\ 0 & e^{-j\theta(t)} \end{bmatrix}, \quad \begin{bmatrix} e^{-j\theta(t)} & 0 \\ 0 & e^{j\theta(t)} \end{bmatrix},$$

respectively. Notice that the multiplications do not commute with the transfer function $\mathrm{diag}\,\{K(s), K(s)\}$.

Let $k(t)$ denote the impulse response of the transfer function $K(s)$. We assume that $K(s)$ is strictly proper for simplicity. The input $\tilde{v}_\alpha(t)$ and the output $\tilde{z}_\alpha(t)$ satisfy

$$\begin{aligned} \tilde{z}_\alpha(t) &= e^{-j\theta(t)} \int_0^t k(t-\tau) e^{j\theta(\tau)} \tilde{v}_\alpha(\tau) d\tau \\ &= \int_0^t k(t-\tau) e^{-j\omega_0(t-\tau)} \tilde{v}_\alpha(\tau) d\tau. \end{aligned}$$

This is the convolution integral whose impulse response is $k(t)e^{-j\omega_0 t}$. Hence its Laplace transformation is $K(s+j\omega_0)$. Similarly, the input $\tilde{v}_\beta(t)$ and the output $\tilde{z}_\beta(t)$ are related by the transfer function $K(s-j\omega_0)$. Hence the system in Fig. 3 shows a time invariant system whose transfer function is $\mathrm{diag}\,\{K(s+j\omega_0), K(s-j\omega_0)\}$.

The input-output relation is recovered by multiplying $\mathrm{diag}\,\{K(s+j\omega_0), K(s-j\omega_0)\}$ with T^{-1} from right and with T from left. Hence

$$\begin{aligned} &T \begin{bmatrix} K(s+j\omega_0) & 0 \\ 0 & K(s-j\omega_0) \end{bmatrix} T^{-1} \\ &= \begin{bmatrix} \frac{K(s+j\omega_0)+K(s-j\omega_0)}{2} & \frac{K(s+j\omega_0)-K(s-j\omega_0)}{2j} \\ -\frac{K(s+j\omega_0)-K(s-j\omega_0)}{2j} & \frac{K(s+j\omega_0)+K(s-j\omega_0)}{2} \end{bmatrix}. \end{aligned} \tag{8}$$

Theorem 1: Assume that the angle of DQ transformation (6) satisfies $\theta(t) = \omega_0 t$ for some ω_0. Then the input-output

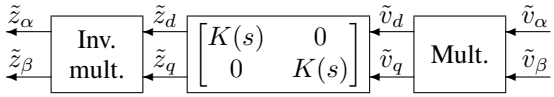

Fig. 3. Diagonalized DQ transformation

relation of Fig. 2 is time-invariant, and its transfer function is given by (8).

Remark 1: In many applications, Fig. 2 is implemented as it is in a device such as FPGA. This requires the multiplication of the rotation matrix and its inverse in real time. Theorem 1 simplifies the implementation without changing the control algorithm.

Remark 2: In [10], a lowpass-bandpass-transformation which is defined by the replacement rule

$$s \rightleftharpoons \frac{s^2+\omega_0^2}{2s}$$

of the Laplace variable is discussed. If the single phase compensator $K(s)$ in Fig. 2 is a PI controller, $K(s) = K_P + K_I/s$, then Theorem 1 shows that the diagonal transfer functions are given by the lowpass-bandpass-transformation. However, the transformation does not explain the off-diagonal transfer functions. Furthermore, if $K(s) = 1/(Ts+1)$, then even the diagonal transfer functions are not given by the lowpass-bandpass-transformation.

Remark 3: The method proposed in [14] is different from ours because it is not based on the analysis of the transformation.

C. Equivalent system – variable angular velocity

In this subsection, the angle $\theta(t)$ in (1), (2), and (3) has a variable angular velocity. Assume that the transfer function $K(s)$ has the state-space representation $K(s) = D + C(sI - A)^{-1}B$. We will find a state-space form of the system in Fig. 2. Note that Fig. 3 is valid even if the angular velocity is not constant.

We may assume that $D = 0$ because the feed-through term of the state space representation in Fig. 3 commute with the multiplication terms. The impulse response of the strictly proper part of $K(s)$ is $Ce^{At}B$, and thus we have

$$\begin{aligned}\tilde{z}_\alpha(t) &= e^{-j\theta(t)}\int_0^t Ce^{A(t-\tau)}Be^{j\theta(\tau)}\tilde{v}_\alpha(\tau)d\tau \\ &= \int_0^t Ce^{At}e^{-j\theta(t)}e^{-A\tau}e^{j\theta(\tau)}B\tilde{v}_\alpha(\tau)d\tau.\end{aligned}$$

Let

$$\tilde{\zeta}_\alpha(t) = e^{At}e^{-j\theta(t)}\int_0^t e^{-A\tau}e^{j\theta(\tau)}B\tilde{v}_\alpha(\tau)d\tau.$$

Then there holds

$$\begin{aligned}\frac{d}{dt}\tilde{\zeta}_\alpha(t) &= \left(A - j\dot{\theta}(t)\right)\tilde{\zeta}_\alpha(t) + B\tilde{v}_\alpha(t), \\ \tilde{z}_\alpha(t) &= C\tilde{\zeta}_\alpha(t).\end{aligned}$$

Similarly, let

$$\tilde{\zeta}_\beta(t) = e^{At}e^{j\theta(t)}\int_0^t e^{-A\tau}e^{-j\theta(\tau)}B\tilde{v}_\beta(\tau)d\tau.$$

Then

$$\begin{aligned}\frac{d}{dt}\begin{bmatrix}\tilde{\zeta}_\alpha(t)\\ \tilde{\zeta}_\beta(t)\end{bmatrix} &= \begin{bmatrix}A - j\dot{\theta}(t) & 0\\ 0 & A + j\dot{\theta}(t)\end{bmatrix}\begin{bmatrix}\tilde{\zeta}_\alpha(t)\\ \tilde{\zeta}_\beta(t)\end{bmatrix} \\ &\quad + \begin{bmatrix}B & 0\\ 0 & B\end{bmatrix}\begin{bmatrix}\tilde{v}_\alpha(t)\\ \tilde{v}_\beta(t)\end{bmatrix}, \qquad (9)\\ \begin{bmatrix}\tilde{z}_\alpha(t)\\ \tilde{z}_\alpha(t)\end{bmatrix} &= \begin{bmatrix}C & 0\\ 0 & C\end{bmatrix}\begin{bmatrix}\tilde{\zeta}_\alpha(t)\\ \tilde{\zeta}_\beta(t)\end{bmatrix}. \qquad (10)\end{aligned}$$

If $D \neq 0$, then (10) becomes

$$\begin{bmatrix}\tilde{z}_\alpha(t)\\ \tilde{z}_\alpha(t)\end{bmatrix} = \begin{bmatrix}C & 0\\ 0 & C\end{bmatrix}\begin{bmatrix}\tilde{\zeta}_\alpha(t)\\ \tilde{\zeta}_\beta(t)\end{bmatrix} + \begin{bmatrix}D & 0\\ 0 & D\end{bmatrix}\begin{bmatrix}\tilde{v}_\alpha(t)\\ \tilde{v}_\beta(t)\end{bmatrix}. \qquad (11)$$

Define the state transformation

$$\begin{bmatrix}\zeta_\alpha(t)\\ \zeta_\beta(t)\end{bmatrix} = T_n\begin{bmatrix}\tilde{\zeta}_\alpha(t)\\ \tilde{\zeta}_\beta(t)\end{bmatrix},$$

where $T_n = T \otimes I_n$, T is defined in (7), $\otimes$ is the Kronecker product, I_n is the n-th order identity matrix, and n is the either size of the rows or columns of the matrix A. Then (9) and (11) become the state equation:

$$\begin{aligned}\frac{d}{dt}\begin{bmatrix}\zeta_\alpha(t)\\ \zeta_\beta(t)\end{bmatrix} &= \begin{bmatrix}A & -\dot{\theta}(t)\\ \dot{\theta}(t) & A\end{bmatrix}\begin{bmatrix}\zeta_\alpha(t)\\ \zeta_\beta(t)\end{bmatrix} \\ &\quad + \begin{bmatrix}B & 0\\ 0 & B\end{bmatrix}\begin{bmatrix}v_\alpha(t)\\ v_\beta(t)\end{bmatrix}, \qquad (12)\\ \begin{bmatrix}z_\alpha(t)\\ z_\alpha(t)\end{bmatrix} &= \begin{bmatrix}C & 0\\ 0 & C\end{bmatrix}\begin{bmatrix}\zeta_\alpha(t)\\ \zeta_\beta(t)\end{bmatrix} + \begin{bmatrix}D & 0\\ 0 & D\end{bmatrix}\begin{bmatrix}v_\alpha(t)\\ v_\beta(t)\end{bmatrix}. \qquad (13)\end{aligned}$$

Hence we have proved the following.

Theorem 2: Assume that the angle $\theta(t)$ of DQ transformation (6) is differentiable. Then the input-output relation of Fig. 2 is linear time varying, and its state-space representation is given by (12),(13).

Remark 4: When the angle velocity is measured, the controller of the form (12),(13) can be implemented as a linear parameter varying (LPV) system.

D. Positive phase sequence and negative phase sequence signals

A three-phase signal is transformed to a two-phase signal using Clarke transformation. When the phase shift of the three-phase signal is in accordance with equations (1), (2), and (3), then the β component of the two phase signal delays $\pi/2$ from the α component as equations (4) and (5) show. This is called a positive phase sequence signal.

A three-phase signal that has the reverse phase delay appears in grid-tie inverter circuits due to disturbances. This subsection analyzes the effect of such a signal. The Clarke transformation of a reverse phase signal yields a two-phase signal:

$$u_{\alpha'} = \sqrt{3}U\sin\left(\theta(t) - \delta\right), \qquad (14)$$

$$u_{\beta'} = \sqrt{3}U\sin\left(\theta(t) - \delta + \frac{\pi}{2}\right). \qquad (15)$$

Fig. 4 shows a feedback system with a disturbance at output. Signals in Fig. 4 are in $\alpha\beta$ domain, and let d denote the disturbance, y the output, r the reference input, and e

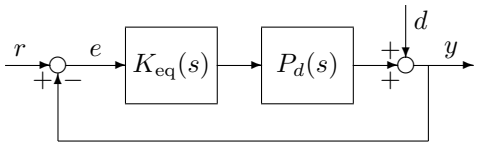

Fig. 4. Feedback system with output disturbance

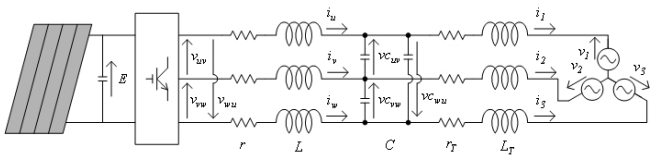

Fig. 5. Grid-tie Inverter Circuits

the tracking error. We assume that the plant P_d is a diagonal transfer function

$$P_d(s) = \begin{bmatrix} P(s) & 0 \\ 0 & P(s) \end{bmatrix},$$

and the controller $K_{\rm eq}$ is given by (8).

If $K_{\rm eq}(s)$ stabilizes the closed loop, then a sinusoidal disturbance results in a sinusoidal output in steady state, which is analyzed using circuit theory. Let $\vec{d}$ and $\vec{y}$ denote the phasors of the sinusoidal signals d and y having α, β components at the angular velocity ω_0, respectively. Then

$$(I + P_d(j\omega_0)K_{\rm eq}(j\omega_0))\,\vec{y} = \vec{d}$$

holds. After an elementary calculation, we find that if $\vec{d}$ is a positive phase sequence signal, then

$$\vec{y} = \frac{1}{1 + P(j\omega_0)K(0)}\vec{d}, \tag{16}$$

and if $\vec{d}$ is a negative phase sequence signal, then

$$\vec{y} = \frac{1}{1 + P(j\omega_0)K(2j\omega_0)}\vec{d}. \tag{17}$$

Note that $\vec{y}$ and $\vec{d}$ are two-dimensional complex vectors.

Remark 5: A single phase compensator in Fig. 1 is usually chosen as a lowpass filter or a PI controller. From (16), we see that the feedback shows high disturbance attenuation ability for a positive phase sequence disturbance. However, it shows relatively low ability for a negative phase sequence unless $K(s)$ has large gain up to the frequency $2\omega_0$ from (17). In order to circumvent the situation, let consider the diagonal transfer function

$$\begin{bmatrix} \frac{K(s+j\omega_0)+K(s-j\omega_0)}{2} & 0 \\ 0 & \frac{K(s+j\omega_0)+K(s-j\omega_0)}{2} \end{bmatrix}, \tag{18}$$

and replace the controller $K_{\rm eq}(s)$ in Fig. 4. Then we see that

$$\vec{y} = \frac{2}{2 + P(j\omega_0)\,(K(0) + K(2j\omega_0))}\vec{d} \tag{19}$$

holds both for positive and negative phase sequence signals instead of (16) and (17). This means that we have the disturbance rejection property if we use the diagonal controller (18) where $K(s)$ is either a lowpass filter or a PI controller.

III. Grid-tie inverter control

A. Controller design

Fig. 5 shows a grid-tie inverter circuits. Using Clarke transformation, a state-space equation is given by

$$\frac{d}{dt}\begin{bmatrix} i_\alpha \\ z_\alpha \\ x_\alpha \\ i_\beta \\ z_\beta \\ x_\beta \end{bmatrix} = \begin{bmatrix} \frac{-r}{L} & 0 & \frac{-1}{L} & 0 & 0 & 0 \\ 0 & \frac{-r_T}{L_T} & \frac{1}{L_T} & 0 & 0 & 0 \\ \frac{1}{3C} & \frac{-1}{3C} & 0 & 0 & 0 & 0 \\ 0 & 0 & 0 & \frac{-r}{L} & 0 & \frac{-1}{L} \\ 0 & 0 & 0 & 0 & \frac{-r_T}{L_T} & \frac{1}{L_T} \\ 0 & 0 & 0 & \frac{1}{3C} & \frac{-1}{3C} & 0 \end{bmatrix}\begin{bmatrix} i_\alpha \\ z_\alpha \\ x_\alpha \\ i_\beta \\ z_\beta \\ x_\beta \end{bmatrix} + \begin{bmatrix} \frac{1}{L} & 0 \\ 0 & 0 \\ 0 & 0 \\ 0 & \frac{1}{L} \\ 0 & 0 \\ 0 & 0 \end{bmatrix}\begin{bmatrix} u_\alpha \\ u_\beta \end{bmatrix},$$

$$\begin{bmatrix} y_\alpha \\ y_\beta \end{bmatrix} = \begin{bmatrix} z_\alpha \\ z_\beta \end{bmatrix},$$

where i_α and i_β are the $\alpha\beta$ components of the three-phase currents i_u, i_v, and i_w, z_α and z_β are the $\alpha\beta$ components of the three-phase currents i_1, i_2, and i_3, x_α and x_β are the $\alpha\beta$ components of the three-phase voltages vc_{uv}, vc_{vw}, and vc_{wu}, and u_α and u_β are the $\alpha\beta$ components of the three-phase voltages v_{uv}, v_{vw}, and v_{wu}, respectively.

Notice that the dynamics of the system for the α and β components are decoupled after Clarke transformation.

The purpose of the control is to maintain the currents i_1, i_2, and i_3 close to the pre-determined sinusoidal reference signal under the disturbance to the circuits. The feedback configuration is given by Fig. 4. We carry out the controller design in the $\alpha\beta$ domain.

We carry out the controller design in the $\alpha\beta$ domain. We apply the H^∞ loop shaping control proposed in [11]. A controller should reject a disturbance having both positive and negative phase sequence signals. Remark 5 suggests that a pre-compensator $W_1(s)$, which is a filter for the loop shaping, is a diagonal transfer function having the form (18), where $K(s)$ is a lowpass filter or a PI controller. We confirm that the design method works using a simulation in Section III-B and an experiment in Section III-C.

B. Simulation

We model a 200 V 5 kW grid-tie inverter whose parameters are given as Table I. The Bode plots of the open loop transfer function from u_α to z_α is shown in Fig. 6. The

TABLE I

GRID-TIE INVERTER PARAMETERS

ω_0 [rad/s]	L [mH]	r [mΩ]	C [μF]	L_T [mH]	r_T [mΩ]
120π	1.2	10	10	0.8	10

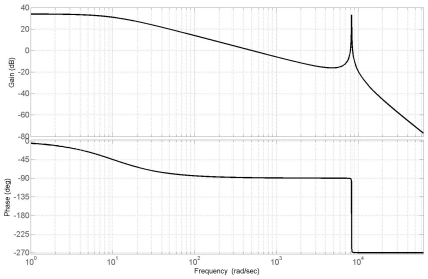

Fig. 6. Bode plot of the plant transfer function

feedback configuration is given by Fig. 4. The reference signal using the $\alpha\beta$ components is

$$r = \begin{bmatrix} 20\cos\omega_0 t \\ 20\sin\omega_0 t \end{bmatrix}.$$

Because of a momentary power interruption, we assume that the feedback loop is subject to a disturbance at the output, whose three-phase components are given as

$$\begin{aligned} d &= d_p + d_n \\ &= \begin{bmatrix} 5\cos\omega_0 t \\ 5\cos\left(\omega_0 t - \frac{2\pi}{3}\right) \\ 5\cos\left(\omega_0 t - \frac{4\pi}{3}\right) \end{bmatrix} + \begin{bmatrix} 10\cos\omega_0 t \\ 10\cos\left(\omega_0 t - \frac{4\pi}{3}\right) \\ 10\cos\left(\omega_0 t - \frac{2\pi}{3}\right) \end{bmatrix}. \end{aligned}$$

The current control system for the grid-tie inverter should satisfy:

1) The output should track the reference signal within 0.1 sec after the feedback system is operational.
2) The disturbance should be rejected within 0.1 sec after it is added to the output.

The weights for the H^∞ loop shaping method [11] are selected as

$$W_1(s) = \begin{bmatrix} \frac{100s}{s^2+\omega_0^2} & 0 \\ 0 & \frac{100s}{s^2+\omega_0^2} \end{bmatrix}, \quad W_2(s) = I.$$

Notice that $W_1(s)$ is of the form (18) with the integral controller $K(s) = 100/s$.

Because the plant and the weights are diagonal, the H^∞ loop shaping controller is diagonal, too, and can be constructed using single-input single-output (SISO) design. A numerical computation shows that the robust stability margin is $\varepsilon_{\max} = 0.644$, which suggest a good design. Fig. 7 shows the Bode plot of the controller.

The controller derived in the preceeding subsection is tested by a simulation study. The disturbance d is added to the output of the system 1 sec after the system is operational. Fig. 8 shows the three-phase signal of the disturbance. Fig. 9 shows the output current for the closed loop during 0 to 0.2 seconds after the system is operational. Fig. 10 shows

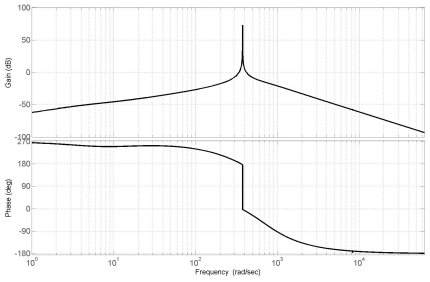

Fig. 7. Bode plot of the controller

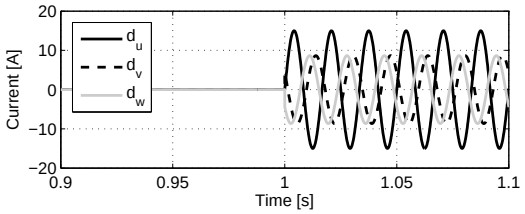

Fig. 8. Disturbance due to a power interruption

the the output current during 0.9 to 1.1 seconds when the disturbance of Fig. 8 is added at the output.

We see that the requirements are fulfilled by the proposed controller. Notice that the negative phase sequence disturbance signal is fairly large. The rejection of such a disturbance was difficult by the conventional controller configuration of Fig. 4.

C. Experiment

We further test our design method by an experiment. A grid-tie inverter used for the experiment is a 100 V inverter and has slightly different parameters than that in Section III-B. We think two kinds of fault;

1) three-phase voltages of the grid drop to 15% of the nominal value for 0.5 seconds due to short-circuit.
2) single-phase voltage of the grid drops to 15% of the nominal value for 0.5 seconds due to two-phase short-circuit without ground contact.

We require that the grid-tie inverter should be operational during the fault, and track the reference current after the grid becomes normal.

Fig. 11 shows the response of the inverter for the three-phase short circuit. We see that the inverter shows no over current during and after the fault and recovers quickly after the grid becomes normal. Fig. 12 shows the response for the two-phase short circuit without ground contact. We see that the inverter works well for this situation, too. Furthermore, we see that during the two-phase short circuit the inverter maintains balanced three-phase currents.

IV. CONCLUSIONS

This paper has discussed a controller design method for a grid-tie inverter achieving FRT capabilities. The method is

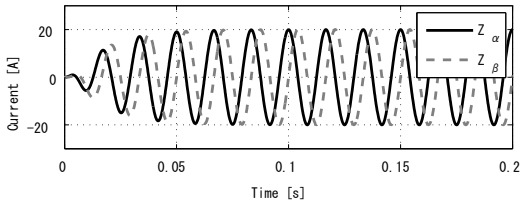

Fig. 9. Output current

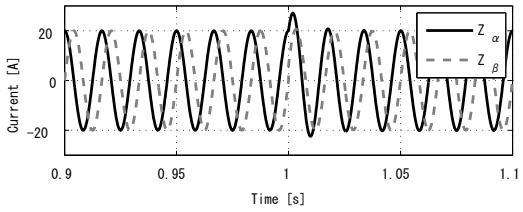

Fig. 10. Output current under disturbance

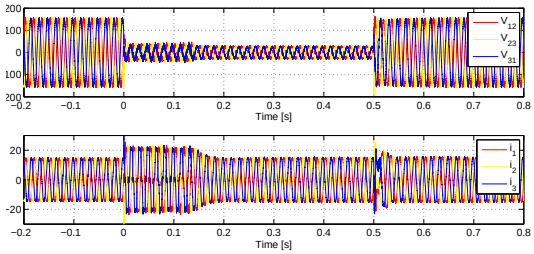

Fig. 11. Grid voltages and inverter currents for three-phase short circuit

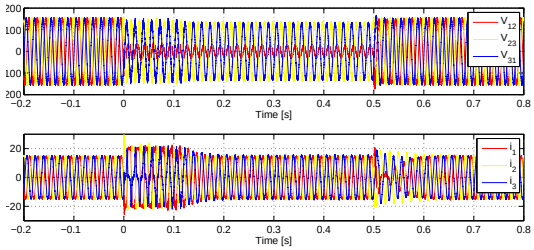

Fig. 12. Grid voltages and inverter currents for two-phase short circuit

based on the analysis of the cascade connection of a diagonal transfer function pre- and post-multiplied by DQ and inverse DQ transformations. The input-output map of the cascade connection is characterized by a transfer function and a state-space representation when the angular velocity is constant and varying, respectively.

The results have been applied for the controller design problem. The transfer function representation of the cascade connection is useful in analyzing the effect of positive phase sequence and negative phase sequence signals. The analysis shows that the conventional configuration using DQ transformation is ineffective for rejecting negative phase sequence disturbance. The proposed method adequately suppresses the negative phase sequence disturbance as was confirmed by a simulation and an experiment. Furthermore, it offers a systematic way to address the control performance using the robust control theory.

ACKNOWLEDGMENTS

This work is supported by The Japan Science and Technology Agency (JST) Strategic Basic Research Programs (CREST) " Creation of fundamental theory and technology to establish a cooperative distributed energy management system and integration of technologies across broad disciplines toward social application."

REFERENCES

[1] State of California, Senate Bill 2, California Renewable Energy Resources Act, http://www.leginfo.ca.gov/pub/11-12/bill/sen/sb_0001-0050/sbx1_2_bill_20110412_chaptered.html

[2] National Policy Unit, Cabinet Secretariat, 14th energy and environment meeting (in Japanese), http://www.kantei.go.jp/jp/topics/2012/pdf/20120914senryaku.pdf

[3] IEEE 1547 Overview, http://www1.eere.energy.gov/solar/pdfs/15_1547.pdf

[4] Colin Schauder, "Impact of FERC 661-A and IEEE 1547 on photovoltaic inverter design," 2011 IEEE Power and Energy Society General Meeting, pp.1–6, 2011.

[5] Energy Networks Association, "Distributed generation connection guide, — A guide for connecting generation that falls under G83/1-1 stage 1 to the distribution network," http://www.energynetworks.org/modx/assets/files/electricity/engineering/distributed generation/DGCG G83 S1 Nov2011.pdf

[6] BDEW, "Generating plants connected to the medium-voltage network," http://www.bdew.de/internet.nsf/id/A2A0475F2FAE8F44C12578300047C92F/$file/BDEW_RL_EA-am-MS-Netz_engl.pdf

[7] Japan Electrotechnical Standards and Codes Committee, Grid-interconnection Code, JESC E0019(2012) (in Japanese), http://www.jesc.gr.jp/jesc-assent/private/jesc_e0019_06r3.html

[8] J. Salaet, S. Alepuz, A. Gilabert, and J. Bordonau, "Comparison between two methods of DQ transformation for single phase converters control Application to a 3-level boost rectifier," 35th Annual IEEE Power Electronics Specialists Conference, pp.214–220, 2004.

[9] M. Gonzalez, V. Cardenas, and F. Pazos, "DQ transformation development for single-phase systems to compensate harmonic distortion and reactive power," IEEE CIEP04, pp.177–182, 2004.

[10] Christian H. Benz, W.-Toke Franke, and Friedrich W. Fuchs, "Low Voltage Ride Through Capability of a 5 kW Grid-Tied Solar Inverter," 14th International Power Electronics and Motion Control Conference, EPE-PEMC 2010, pp.T12-13–T12-20, 2010.

[11] D.C. McFarlane and K. Glover, "A loop shaping design procedure using H_∞ synthesis," IEEE Transactions on Automatic Control, vol.37, no.6, pp.759–769, 1992.

[12] W. C. Duesterhoeft, Max W. Schulz, and Edith Clarke, "Determination of instantaneous currents and voltages by means of alpha, beta, and zero components," Transactions of the American Institute of Electrical Engineers, vol.70, no.2, pp.1248–1255, 1951.

[13] R. H. Park, "Two-reaction theory of synchronous machines: generalized method of analysis - part I," Transactions of the American Institute of Electrical Engineers, vol. 48, pp.716–730, 1929.

[14] Wonhee Kim, Chuan Yang, and Chung Choo Chung, "Design and implementation of simple field-oriented control for permanent magnet stepper motors without DQ transformation," IEEE Transactions on Magnetics, Vol.47, No.10, pp.4231-4234, 2011.